JOURNAL OF APPLIED POLYMER SCIENCE VOL. 21, 2359–2373 (1977)

Kinetics of Epoxy Resin Polymerization Using Differential Scanning Calorimetry

P. PEYSER and W. D. BASCOM, *Naval Research Laboratory, Surface Chemistry Branch, Code 6170 Chemistry Division, Washington, D.C. 20375*

Synopsis

The kinetic parameters of the polymerization of diglycidyl ether of bisphenol A with hexahydrophthalic anhydride and benzyldimethylamine as catalyst were determined using differential scanning calorimetry. The reaction was found to be first order with some variation with temperature, and the activation energy and natural log of the frequency factor were 25 kcal/mole and ~25 sec^{-1}, respectively. These results are discussed with respect to a steady-state mechanism of the polymerization and compared with results reported for other epoxide–anhydride reactions.

INTRODUCTION

An earlier paper[1] reported a differential scanning calorimetry (DSC) determination of the kinetics of polymerization of diglycidyl ether bisphenol A (DGEBA) with "nadic" methyl anhydride (NMA) and benzyldimethylamine (BDMA) as catalyst. Data analyses for the activation energy, reaction order, and frequency factor were carried out using four computational methods. The results indicated a two-stage polymerization process: an initial relatively slow reaction which after about 12% completion was followed by a sharp increase in both rate and activation energy.

In this report, a study of the DGEBA–hexahydrophthalic anhydride (HHPA) polymerization kinetics with BDMA as catalyst is described. The two anhydrides, NMA and HHPA, are chemically similar except that HHPA is a solid at room temperature. Also the effect of amine concentration and exploratory work on the effect of a silica filler on the kinetics are reported.

Data analyses of the DSC results indicate that the kinetics of the DGEBA–HHPA system differs significantly from those of the NMA–DGEBA reaction despite the similarities of the two anhydrides. The analyses were performed using the previously described methods.[1] In addition, new methods are presented for data analysis of the effect of variation in frequency factor and for determining the reaction order from isothermal DSC experiments.

EXPERIMENTAL

The procedures used in this study were essentially the same as those previously described.[1] The DGEBA (diglycidylether bisphenol A, DER 332, Dow Chemical Co., epoxy equiv. = 175) and HHPA (hexahydrophthalic anhydride, Matheson,

Coleman and Bell, mp 35–36°C) were used as received. Prior to mixing, the reactants were melted at ~50°C. A white, insoluble precipitate of unknown composition settled out of the liquid HHPA and was separated by decantation. Test DSC samples were prepared by mixing equivalents of epoxide and anhydride and stirring at slightly above ambient (~25°C) temperature for 10 min to give a clear, slightly yellowish solution. The BDMA (benzyldimethylamine, 98%, Eastman Organic Chemicals) was then added from a microsyringe to the solution and stirring was continued for another 15 min. At this point, the solution became yellow-brown in color. Ten to 40 mg was transferred to aluminum micropans, covered, and placed in a Perkin-Elmer DSC-2. The instrument had been preset at 315°K. After 10 min at 315°K, the sample was either heated to 500°K at 0.3125°K/min or 1.25°K/min (dynamic tests) or rapidly heated (320°K/min) up to a predetermined temperature (isothermal tests). Difficulties encountered earlier[1] with condensate forming on the pan covers were not evident here. The DSC output (change in heat content per unit time, dH/dt) was digitally recorded along with the temperature and time elapsed using a Digitem Model DAS-1A data logger. The experimental output was corrected for instrumental baseline shift by a point-by-point subtraction of the output for two empty pans run against each other. A computer program was used to smooth the data, to connect the initial and final baselines by an iterative process (in which it was assumed the baseline changed in proportion to the fraction reacted), and to analyze the data according to the various DSC kinetic equations described in the next section. The baseline for the isothermal data was established by back extrapolating the final data points which after the reaction was completed were essentially constant with time.

The silica filler (Cabosil, Cabot Corp.) had a nominal surface area (BET) of 150–200 m^2/g. The powder was heated overnight in a muffle oven at 500–720°C to remove physically (H-bonded) adsorbed water and probably some chemically absorbed water as well.[2] After cooling, weighed portions of the silica were added to the epoxy–anhydride–catalyst mixture. To assure realistic comparison, DSC runs were conducted on unfilled samples of the same epoxy mixture used to prepare the silica filled samples.

DATA ANALYSIS

The mathematical methods of obtaining kinetic information from thermogravimatric analysis (TGA) are applicable to DSC data. Except when noted, the methods described here are discussed in the review on TGA analysis by Flynn and Wall.[3] In using these analyses, it is assumed that the reactions can be described by a simple nth order, Arrhenius-type temperature dependence. Such an assumption is not usually justified for complex plymerizations, especially in the latter stages of reaction. However, in the system studied here, the reaction appears to follow simple Arrhenius kinetics through at least 75% completion (see Fig. 1).

Dynamic Studies

The assumption is made that the extent of reaction is proportional to the heat evolved, so that the Arrhenius equation becomes

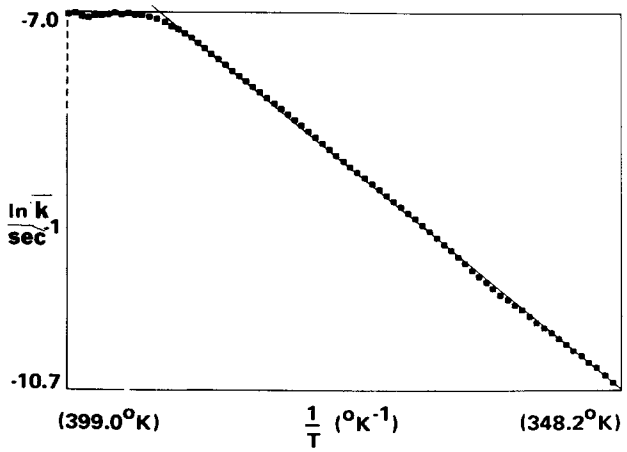

Fig. 1. Equation (1b) plot of DSC data for a single dynamic run. Solid line is least-squares fit.

$$\frac{1}{H_T}\frac{dH}{dt} = Ae^{-E_a/RT}f\left(\frac{H}{H_T}\right) = Ae^{-E_a/RT}\left(\frac{H_T - H}{H_T}\right)^n \tag{1a}$$

or, in the more useful logarithmic form,

$$\ln\frac{dH}{dt}\frac{1}{H_T} - n\ln\frac{H_r}{H_T} = -\frac{E_a}{RT} + \ln A \equiv \ln k \tag{1b}$$

where H_T = total heat of reaction (cal/g) ~ area under DSC curve; $H_r = H_T - H$; H = heat of reaction at a given time and temperature ~ partial area under curve; E_a = Arrhenius activation energy (kcal/mole); A = Arrhenius equation frequency factor; n = order of reaction; R = gas constant; T = temperature (°K); and $f(H/H_T)$ = a function of H_T which is assumed here to be $(H_r/H_T)^n$. If the reaction order n is either known or assumed, then a plot of ln k, i.e., LHS of eq. (1b), against $1/T$ gives a straight line of slope E_a and intercept ln A.

DSC data can be treated using alternate forms of eq. (1) evaluated at variable heating rate but under conditions of constant temperature or constant fraction reacted. In so doing, expressions are obtained which can be used to establish the uniqueness of the kinetic parameters which were obtained from applying eq. (1) to data for a single heating rate. In the remainder of this section, various of these relationships are described, but a more complete discussion can be found in references 1 and 3.

The maximum point of a DSC curve, dH/dt versus T, can be used to obtain the ratio E_a/n from the expression

$$\frac{E_a}{n} = \left[\left(\frac{RT^2}{(H_T - H)\beta}\right)\frac{dH}{dt}\right]_{(dH/dt)\max} \tag{2}$$

where β is the heating rate. The reaction order n can be obtained independently using

$$(1-\alpha)_{\max} = e^{-r_2} \qquad n = 1 \tag{3a}$$

$$(1-\alpha)_{\max} = \left[\left(\frac{1-n}{n}\right)r_2 + 1\right]^{1/(n-1)} \qquad n \neq 1 \tag{3b}$$

where $\alpha = H/H_T$ (fraction reacted) and r_2 is a second-order correction derived from a series solution of the integral form of the rate equation. The term r_2 approaches 1 as E_a/RT approaches infinity. Values of r_2 as a function of E_a/RT can be obtained from Table I of reference 3.

The Freeman-Carroll (FC) methods of analysis[3,4] permit the simultaneous determination of both activation energy and reaction order, and the form of the FC equation used here was

$$\frac{\Delta \ln dH/dt}{\Delta \ln H_r} = \frac{(E_a/R)\,\Delta\, 1/T}{\Delta \ln H_r} + n. \tag{4}$$

The activation energy can be obtained by comparison at equal fraction reacted of two DSC scans at different heating rates, i.e.,

$$\left(\frac{\Delta \ln \dfrac{dH}{dt}\dfrac{1}{H_T}}{\Delta\, 1/T}\right)_\alpha = -\frac{E}{R} \tag{5a}$$

Assuming that the fraction reacted is the same at the maximum point of DSC curves regardless of the heating rate, then, from (2) and (5a),

$$\left(\frac{\Delta \ln (\beta/T^2)}{\Delta\, 1/T}\right) = -\frac{E_a}{R} \tag{5b}$$

Equations (5a) and (5b) are valid only if the frequency factor A is constant for the different DSC runs. (In the study of reference 1, it was incorrectly assumed that (5b) is valid even if A changed between runs. This error did not affect the conclusions reported.) A more general form of (5a) is

$$\left(\frac{\Delta \ln \dfrac{dH}{dt}\dfrac{1}{H_T}}{\Delta\, 1/T}\right)_\alpha = -\frac{E_a}{R} + \frac{\Delta \ln A}{\Delta\, 1/T} \tag{6a}$$

and, if evaluated at the maximum point,

$$\left(\frac{\Delta \ln (\beta/T^2)}{\Delta\, 1/T}\right) = -\frac{E_a}{R} + \frac{\Delta \ln A}{\Delta\, 1/T} \tag{6b}$$

A similar formalism can be derived for two runs of different heating rates compared at the same temperature. In general form,

$$n_a \equiv \left(\frac{\Delta \ln d\alpha/dt}{\Delta \ln (1-\alpha)}\right)_T = n + \left(\frac{\Delta \ln A}{\Delta \ln (1-\alpha)}\right)_T \tag{7}$$

where n_a is the apparent reaction order. All of these expressions, (6a), (6b), and (7), can be derived from (1b) by subtracting one run from another at constant α or T. A plot of the LHS of (7) against $1/\Delta \ln (1-\alpha)$ gives a straight line of slope $\Delta \ln A$ and intercept n. Use of eq. (7) gives more accurate results than (6a) or (6b) since the variable in the latter, $\Delta(1/T)$, is nearly constant at constant α. However, if $\Delta \ln A$ is known independently, then (6b) is a convenient means for computing the activation energy.

Isothermal Studies

Difficulties in analysis of isothermal DSC runs arise because of uncertainties in the initial 10% of the scan as the sample is rapidly heated to the test temperature. Consequently, the total heat evolution, H_T, is not known with sufficient accuracy. On the other hand, H_r, the heat evolution from any time after the initial equilibration to the end of the reaction ($H_T - H$), can be determined accurately. Equation (1b) can be transformed to

$$\ln\left(\frac{1}{H_T}\frac{dH}{dt}\right) = n \ln\left(\frac{H_T - H}{H_T}\right) + \ln k \tag{8}$$

so that a linear plot of ln (dH/dt) versus ln H_r will have a slope of n and an intercept of ln k + (1 − n) ln H_T. Note that H_T need not be known to determine n. On the other hand, if H_T is known or can be reasonably estimated and ln A does not change between runs, then a plot of ln k versus $1/T$ for runs at different isothermal temperatures gives the activation energy. The linearity of the plot of eq. (8) provides a test of whether the reaction is following simple, eq. (1), isothermal kinetics.

RESULTS

The reaction conditions for the DSC experiments are given in Table I along with the heats of reaction. The values of the latter were reasonably constant despite the variation in sample size, heating rate, amine concentration, etc.

Data analysis using eq. (1b) is illustrated by the plot in Figure 1 for experiment A. The solid line represents the least-squares fit to that portion of the data used for analysis. This plot is typical of the results obtained and indicates the accu-

TABLE I
Sample Parameters

Experiment	Heating rate, °K/min	BDMA, ml/g[a]	Sample weight, mg	Weight fraction of Cabosil	Heat of reaction, cal/g
		Dynamic experiments			
A	0.3125	0.00338	47.33	—	83.7
B	0.3125	0.00338	31.91	—	77.3
C	1.25	0.00338	15.04	—	82.5
D[b]	1.25	0.00338	17.01	—	~71.2
E[b]	1.25	0.00338	32.76	0.05	~87.1
F[b]	1.25	0.00338	21.64	—	80.5
G[b]	1.25	0.00338	28.09	0.06	85.2
H	0.3125	0.00166	29.01	—	87.4
I	0.3125	0.00076	19.66	—	85.7
	Temp., °K	Isothermal experiments			
J	400	0.00338	33.05	—	~78.2
K	415	0.00338	26.57	—	~84.1
L	430	0.00338	33.49	—	~75.9

[a] ml BDMA/g of (DER + HHPA).

[b] D and E are pairs and F and E are pairs. Pairs were from the same sample and were scanned in close proximity, timewise.

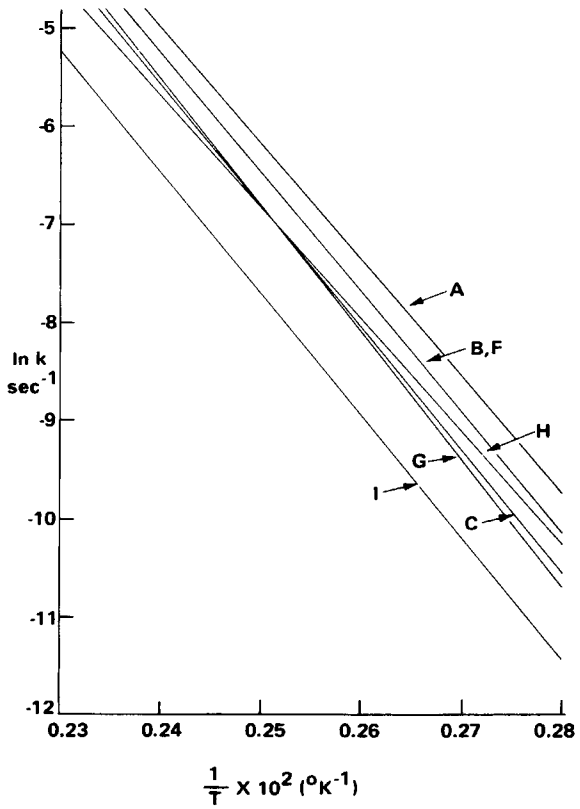

Fig. 2. Least-squares plots of DSC dynamic run data. See Table I for sample composition and Table II for kinetic parameters derived from these plots.

racy of the least-squares fit. In this plot and all other computations using eq. (1b), it was assumed that n was unity.

The effects of amine concentration and heating rate on the reaction rate are shown in Figure 2 by least-squares plots of eq. (1b). Note that the lines are reasonably parallel indicating that the activation energy was more or less constant. However, the lines did not superimpose on each other, even when the amine contents and the heating rates of the experiments were the same, e.g., experiments A and B. Inspection of eq. (1b) suggests that differences in the frequency factor could cause the plots to be parallel but shifted along the ln k axis.

The values of E_a and ln A obtained from the least-squares plots of the data fitted to eq. (1b) are listed in Table II along with the least-squares regression coefficient, and the range of fraction reacted over which the data were linear for each experiment. The ln A values obtained by extrapolation to $1/T = 0$ are only approximate since slight variations in line slope well within experimental precision would severely affect the long extrapolation. For example, compare experiments A and I which gave the same values of ln A, yet in Figure 2 are considerably displaced from each other.

The results of data analysis from the maximum points of the DSC curves are listed in Table III. The E_a/n values were obtained using eq. (2) and the n values in the fifth column from eqs. (3a) and (3b). These latter results are probably

inaccurate since the maxima of the DSC curves were rather broad as evidenced (Table III) by the range in temperature and fraction reacted near the maximum points. A somewhat more accurate estimate of n was made using the values for E_a in Table II and E_a/n in Table III, and the results are listed in column six of Table III.

The reaction order was determined directly using eq. (7) which compares the fraction reacted for two DSC scans at fixed temperature. The equation is simplified if the frequency factor is constant between the two runs. This appears to be the case for experiments B and F, since their least-squares plots in Figure 1 are quite close. In Table IV, the values of n calculated for this pair of experiments are given along with the temperatures at which they were compared and the corresponding fraction reacted. The results indicate first-order kinetics in agreement with the other analyses (Table III).

Comparison of other pairs of DSC scans required the use of the full form of eq. (7) since $\Delta \ln A$ could not be assumed to be zero. In Figures 3 and 4, linear plots of eq. (7) for various pairs of experiments are seen to intercept the axis at $n = 1$. The slope of these plots gives $\Delta \ln A$ for each pair of experiments and the values obtained were equal to the separation along the ordinate axis of the parallel lines of Figure 3. The $\Delta \ln A$ values did not correlate with the $\ln A$ values of Table II because of the large extrapolation error mentioned earlier. Not all experimental pairs gave linear Plots of eq. (7), e.g., experiments I and H in Figure 3. These two runs had a greater difference in slope in the eq. (1b) plots of Figure 3 than the other pairs, indicating an experimental difference in E_a, and the derivation of eq. (7) assumes that the E_a values of the two experiments are not significantly different.

The value of $\Delta \ln A$ obtained in comparing experiments A and C (Fig. 4) was used to compute E_a from eq. (6b), and the results listed in Table V agree with the results in Tables II and III.

The Freeman-Carroll, eq. (4), results for E_a and n are given in Table VI and are essentially identical to those obtained by the other analysis methods. Note in Table VI that the ratio E_a/n is more nearly constant for the different experiments than either of the parameters alone. This difference arises because errors in the slope of these plots tend to change E_a and n in the same direction.

Usually, the dynamic runs gave no indication of a change in reaction rate at

TABLE II
Data Analysis Using Equation (1b)[a]

Experiment	Activation energy, kcal/mole	$\ln A$, sec^{-1}	Range of linearity (fraction reacted)	Regression coefficient
A	23.8	23.8	0.004–0.86	0.9999
B	24.3	24.1	0.010–0.92	0.9997
C	25.0	24.6	0.030–0.98	0.9990
D	~27.1	~27.4	0.015–0.75	0.9990
E	~25.8	~25.8	0.12–0.72	0.9992
F	24.5	24.3	0.12–0.80	0.9997
G	25.9	25.8	0.018–0.75	0.9980
H	22.8	21.9	0.080–0.94	0.9992
I	24.9	23.6	0.045–0.79	0.9996
Average	24.9 ± 1.26			

[a] Assume $n = 1$.

the start of the reaction. However, for experiment I (Fig. 5), where the amine concentration was the lowest and the reaction rate was the slowest, a slight indication of a change in reaction rate at very low values of α was found. Clear indications of an increase in reaction rate at the start of the reactions was found for the isothermal runs, as can be seen from Figure 6 in which the reaction rate is plotted versus ln H_r, eq. (8). (Note that time increases from right to left in Figure 6.)

The isothermal data can be used to compute ln k from eq. (8) if it can be assumed that H_T can be determined accurately and ln A is constant. Since the range of isothermal temperatures was chosen not to be so high that the beginning of the reaction was obscured nor so low that the reaction could not go to completion, it is likely that the total heat of reaction, H_T, can be reasonably estimated from the isothermal scan results. As for ln A, the samples used for the isothermal runs were taken from a single batch of reactant mixture. This procedure differs from that of the dynamic scan experiments where a new batch was mixed each time to avoid any possible aging effects. This problem was less severe for the isothermal experiments since the runs took much less time than the dynamic scans. It is judged that the variation in ln A in the dynamic experiments was due to using different reactant batches; and, if so, ln A may have been relatively constant for the three isothermal runs.

The values of ln k obtained using eq. (8) were plotted against $1/T$ as in Figure 7. Initially, the reaction order n in eq. (8) was assumed to be 1, but the slope E_a obtained from the Arrhenius plot gave an anomalously low value of ~14 kcal/mole, significantly less than the 25 kcal/mole from the dynamic experiments. On the other hand, when the experimental values of n (Fig. 6) were used to compute ln k, the Arrhenius plot (Fig. 7) gave E_a = 21 kcal/mole, quite consistent with the dynamic results.

TABLE III
Data Analysis Using Equations (2), (3a), and (3b)

Experiment	Maximum temp., °K	Fraction reacted at max.	E_a/n, kcal/mole[a]	n ($3a$ + $3b$)	n[b]
A	378.5–381.0	0.56–0.64	23.1	1.28–0.85	1.03
B	383.3–386.0	0.58–0.67	25.4	1.16–0.73	0.96
C	402.0–404.0	0.56–0.62	23.4	1.28–0.95	1.07
I	386.6–389.7	0.59–0.68	24.1	1.10–0.69	0.95
J	398.0–401.0	0.59–0.68	25.4	1.10–0.69	0.98

[a] Calculated from the midpoint of the maximum temperature range.
[b] Calculated from E_a/n (column 4) and E_a of Table II.

TABLE IV
Equation (7) Applied to Experiments B and F (Δ ln A = 0)

$(1-\alpha)_F$	$(1-\alpha)_B$	T, °K	n
0.798	0.406	383.5	1.04
0.704	0.247	388.5	0.99
0.584	0.117	383.4	1.00
0.407	0.033	399.6	1.12

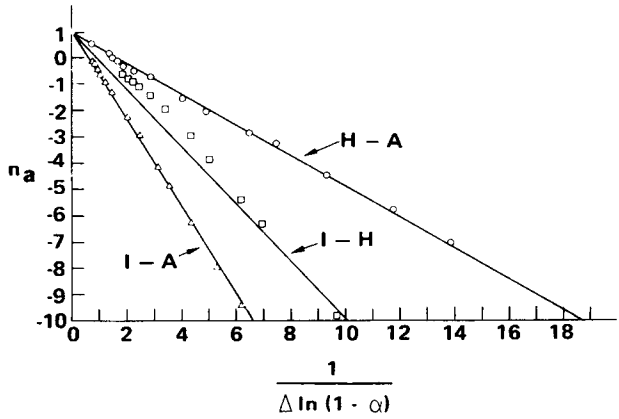

Fig. 3. Comparison of pairs of DSC dynamic runs at constant temperature using eq. (7).

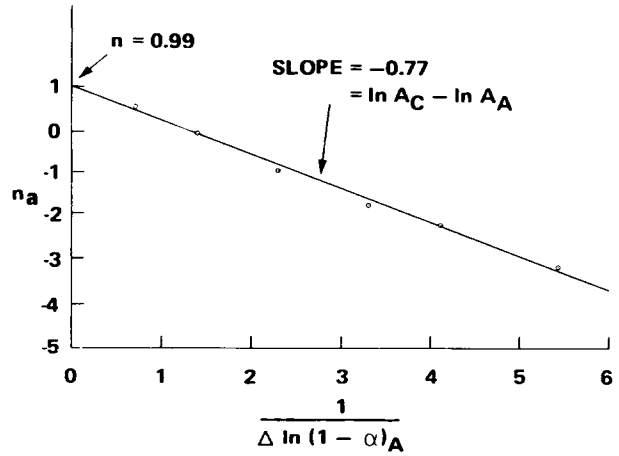

Fig. 4. Comparison of DSC dynamic runs A and C at constant temperature using eq. (7).

There was no discernible effect of adding silica filler to the reaction mixture (compare experiments D with E and F with G in Tables II and VI), and the matter was not pursued further.

DISCUSSION

The mechanisms of epoxy–anhydride polymerizations in the presence of a tertiary amine catalyst are unquestionably complex and by no means fully understood. However, there is more-or-less general agreement that a cocatalyst is involved such as water, alcohols, phenols, or other H-bonding agents present as contaminants in the reactants. Thus, Tanaka et al.[5,6] propose a catalyst activation step

$$\underset{C_A}{R_3N} + \underset{C_{HA}}{HA} \underset{k_2}{\overset{k_1}{\rightleftharpoons}} \underset{C_E}{[R_3N \ldots . HA]} \qquad \text{(a)}$$

to form an initiator. Tanaka and Kakiuchi[6] suggest the formation of α,β-unsaturated alcohols as cocatalysts by the action of the tertiary amine on the ep-

oxide, in addition to contaminants. In the mechanism proposed by Feltzin et al.,[7] a similar activation step is visualized. Following catalyst activation, the complex is believed to associate with either the epoxy or anhydride as in the mechanism of Tanaka and Kakiuchi:[8]

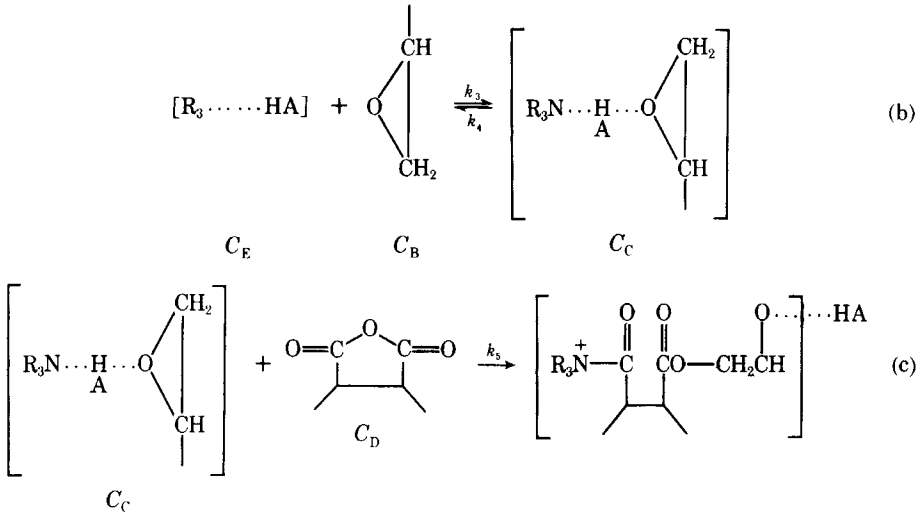

(b)

(c)

TABLE V
Determination of Activation Energy from Experiments A and C using Equation (6b) and $\Delta \ln A$ from Figure 5

α	E_a/R uncorrected	E_a/R corrected	E_a, kcal/mole
0.1	7.36×10^3	12.35×10^3	24.5
0.2	7.84×10^3	12.71×10^3	25.3
0.3	8.20×10^3	13.08×10^3	26.0
0.4	8.31×10^3	13.25×10^3	26.3
0.5	8.33×10^3	13.29×10^3	26.4
0.6	8.41×10^3	13.40×10^3	26.6
0.7	8.39×10^3	13.40×10^3	26.6
0.8	8.43×10^3	13.45×10^3	26.7
		Average	26.0 ± 0.77

TABLE VI
Freeman-Carroll Method

Experiment	Activation energy E_a, kcal/mole	n	E_a/n	Range of α	Regression coefficient
A	26.2	1.18	22.2	0.10–0.86	0.997
B	25.4	1.18	21.5	0.04–0.97	0.954
C	25.3	1.20	21.1	0.03–0.98	0.954
F	25.0	1.09	23.0	0.12–0.83	0.999
G	26.3	1.11	23.8	0.13–0.75	0.997
H	21.9	0.96	22.8	0.13–0.94	0.981
I	27.2	1.29	21.0	0.07–0.57	0.979
	Average	1.14 ± 0.10	22.2 ± 2.2		

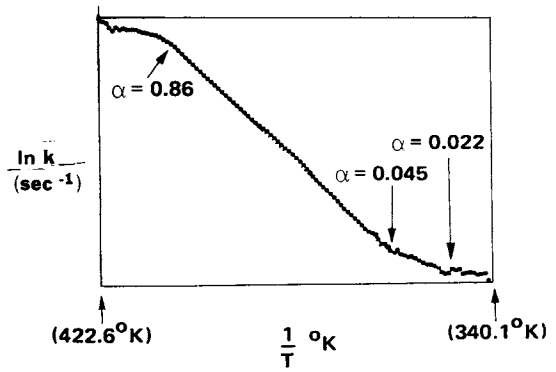

Fig. 5. DSC dynamic data plot of eq. (1b) for a sample with low amine concentration (experiment I).

which is modified here to meet the more recent conclusion[5,6] that the attack of the activated complex is on the epoxide rather than the anhydride. They assume a steady-state condition such that $dC_E/dT = dC_C/dT = 0$ and obtained the rate equation

$$v = \frac{dC_B}{dt} - \frac{k_1k_3k_5C_AC_BC_DC_{HA}}{k_2k_4 + k_2k_5C_D + k_3k_5C_BC_D}$$

Depending upon which of the reaction steps is rate determining, a variety of kinetics are possible. If the formation of activated complex is slow (k_5 and $k_3 \gg k_2, k_4$), then

$$v = k_1C_AC_{HA}$$

and the reaction rate is dependent only on the catalyst (and cocatalyst) concentration. Feltzin et al.[7] found this to be the case in their study of the DGEBA/NMA/BDMA system. On the other hand, if reactions of type b are controlling ($k_3, k_4 \ll k_2$), then

$$v = -\frac{k_1k_3}{k_2}C_AC_{HA}C_D$$

and the rate is first order with respect to epoxy concentration, as was found here and for the initial stages of the DGEBA/NMA/BDMA system. Tanaka and Kakiuchi found second-order kinetics[8] for a variety of epoxy–anhydride systems and suggested that reactions of type C were rate controlling ($k_1 > k_2,k_3,k_4 > k_5$) so that

$$v = -\frac{k_1k_3k_5}{k_2k_4}C_AC_BC_DC_{HA}$$

The monomer–time consumption curves for epoxy/anhydride/amine reactions have been generally found to be sigmoidal in shape, indicating an accelerating reaction over as much as 50% of the reaction time.[8] The curves of Feltzin et al.[7] for the DGEBA/NMA/BDMA indicate an initial accelerating stage, as do those of Fava[9] for the DGEBA/HHPA system catalyzed with tris-2,4,6-dimethylaminomethylphenol. An early accelerating stage was observed here in the first 5–10 min of the isothermal experiments (Fig. 7) and in the dynamic scan at low amine

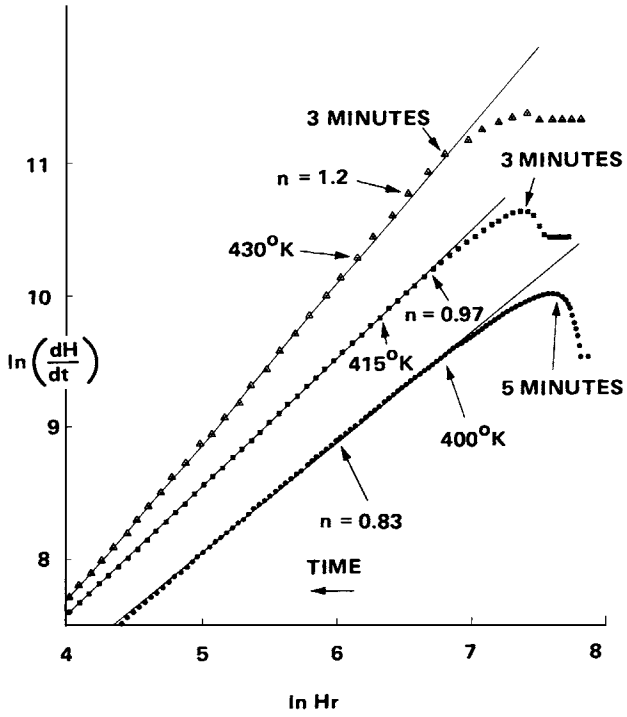

Fig. 6. DSC isothermal data plots of eq. (8).

concentration. Quite possibly, this initial stage represents an induction period in which the reaction is reaching the steady-state condition. Evidently, the induction period for the DGEBA/HHPA/BDMA system is so short as to be undetectable in dynamic DSC experiments if the catalyst concentration is sufficiently high. In support of this argument, the consumption–time curves given by Tanaka and Kakiuchi[8] for epoxy–anhydride reactions catalyzed by BDMA indicate that the induction periods were much shorter than for reactions with most other catalysts.

In view of the complexity of the epoxy–anhydride polymerization, it is not surprising that studies of the reaction kinetics have such a diversity in the observed kinetic parameters. Some of the results to be found in the literature are listed in Table VII. The reaction orders of 0, 1, and 2 predicted by the steady-state kinetics are reported along with activation energies of 12–38 kcal/mole. In two instances, the rate-controlling step was found to change during the course of the reaction. Tanaka and Kakiuchi[8] found that the reactions in nonaqueous media of substituted phenyldiglycidyl ethers with HHPA catalyzed by *t*-butylamine were initially controlled by reaction step b and that the rate increased (autocatalysis) with the buildup of such specie as C_C until the formation of the activated complex, reaction a, became rate controlling. Peyser and Bascom[1] found the kinetics of the DGEBA/NMA/BDMA system to be initially first order and persumably controlled by type b reactions, but then to exhibit second-order kinetics indicating control by type c reactions. Actually, the process probably becomes diffusion controlled since a large increase in activation energy accompanied the change in reaction order. This change to diffusion control did not

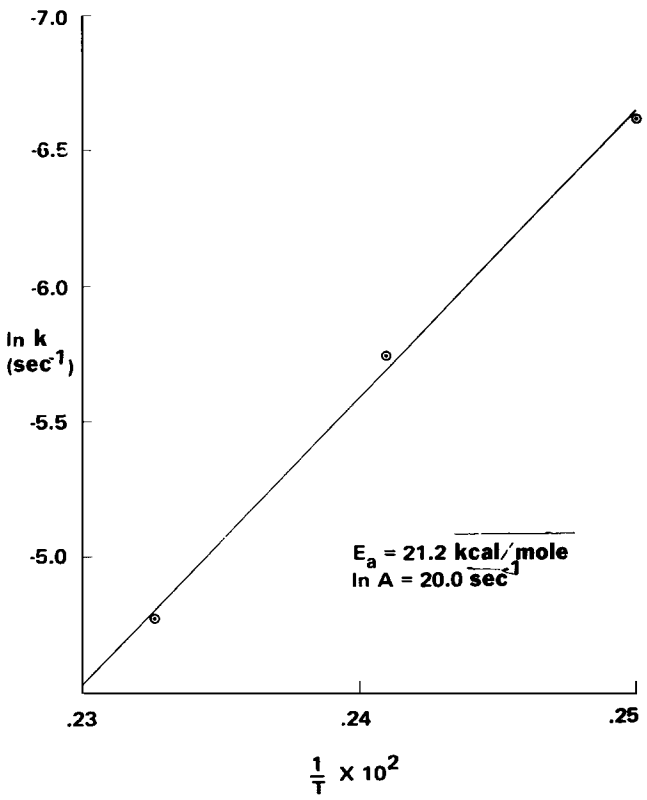

Fig. 7. Arrhenius plot of isothermal DSC data but including the change in reaction order with temperature.

occur for the HHPA-cured system possibly because of the smaller molecular size compared to NMA. Measurements of molecular models indicate the rotational volume swept by the NMA to be 75% greater than for the HHPA.

In view of the important role of cocatalysts in the reaction mechanism, it is quite likely that contaminants such as water or low molecular weight acids and bases can decisively affect the reaction kinetics. This problem is especially acute when studying industrial-grade materials which are difficult to impossible to adequately purify. A case in point is the NMA curing agent which is available only as a technical-grade material, and this may explain the very different results obtained by Feltzin et al.[7] compared to Peyser and Bascom[1] in their studies of the DGEBA/NMA/BDMA polymerization (Table VII).

Part of the discrepancy in the activation energies of Table VII may lie in the indiscriminate use of Arrhenius plots. As was previously mentioned in connection with the isothermal experiments, a small systematic change in the reaction order with temperature has a large effect on the slope of ln k-versus-$1/T$ plots. Also, the dynamic experiment results are affected by a change in n with T although to a lesser degree than the isothermal results. The computations listed in Table VIII show that a change of n in the range of 1.0 to 1.5 does not detectably affect the linearity of the dynamic ln k-versus-$1/T$ plots or the ratio E_a/n. There is, however, a variation in E_a due to the $n(\ln H_r)$, i.e., $(1-\alpha)^n$, term in eq. (1b). This term has a relatively small effect in the early stages of the reaction ($\alpha < 0.5$); and for this reason, the variation in n has a less severe effect on

the dynamic results than on the isothermal results. Ideally, the variation of n with T could be determined from the isothermal study and used as a correction for the dynamic scan data.

SUMMARY

The kinetics of the polymerization of the DGEBA/HMPA/NMA system were determined using DSC. The results of both dynamic and isothermal scans were subject to extensive data analysis. The dynamic experiments indicated the reaction to be approximately first order and the activation energy and natural log of the frequency factor found to be 25 kcal/mole and ~25 sec^{-1}, respectively. The isothermal results indicated first-order kinetics with some variation with temperature and an activation energy of 22 kcal/mole.

These results are consistent with the generally accepted steady-state mechanism of the epoxide–anhydride polymerization reaction. Actually, this reaction mechanism predicts zero-, first-, and second-order kinetics depending on the experimental conditions; and inspection of the results reported in the literature indicates that all three have been observed for various epoxide–anhydride systems. Discrepancies in the reported values for the activation energies may be partly due to incorrectly assuming that the reaction order is constant.

TABLE VII
Kinetic Parameters Obtained for Various Epoxy Resin Polymerizations

Anhydride	Epoxide	Catalyst	Reaction order n	E_a, kcal/mole	ln A, sec^{-1}	Reference
HHPA	DGEBA	BDMA	~1	25	27	this work
HHPA	cyclo-aliphatic	BDMA–ethylene glycol	—	12.2	—	9
HHPA	DGEBA	DMAMP[a]	—	17.8	—	8
HHPA	PGE[b]	*t*-butylamine	1 (initial)[c]	13.6–14.8	9.1–9.9	5
			0 (maximum)[c]	17.6–12.9	9.1–9.5	
NMA	DGEBA	BDMA	0[d]	13.2	16.5	6
NMA	DGEBA	BDMA	1 (initial)	15	10.5–11.1	1
			2 (final)	38	38.0–46.1	

[a] Tris-2,4,6-dimethylaminemethylphenol.

[b] Substituted phenyldiglycidyl ethers.

[c] Initial stage, second order with respect to epoxide and amine catalyst; at maximum rate, first order with respect to catalyst.

[d] First order with respect to catalyst.

TABLE VIII
Effect of Varying n on E_a and ln A Calculated from Equation (1b)[a]

Assumed n	E_a, kcal/mole	E_a/n	ln A	Regression coefficient
2	39.6	19.8	46.0	0.972
1.5	30.7	20.5	33.5	0.994
1.4	28.9	20.6	31.0	0.996
1.3	27.1	20.9	28.4	0.997
1.25	26.2	21.0	27.2	0.998 (max)
1.2	25.3	21.1	25.9	0.997
1.1	23.5	21.4	23.4	0.993
1.0	21.8	21.8	20.9	0.985

[a] Data taken from experiment A in the α = 0.03 to 0.97 range.

References

1. P. Peyser and W. D. Bascom, in *Analytical Chemistry*, Vol. 3, R. S. Porter and J. F. Johnson, Eds., Plenum Press, New York, 1974, p. 537.
2. W. D. Bascom, *J. Phys. Chem.*, **76,** 3188 (1972).
3. J. H. Flynn and L. A. Wall, *J. Res. Natl. Bur. Stand.*, **70A,** 487 (1966).
4. E. S. Freeman and B. Carroll, *J. Phys. Chem.*, **62,** 394 (1958).
5. Y. Tanaka and T. F. Mika, in *Epoxy Resins*, C. A. May and Y. Tanaka, Eds., Marcel Dekker, New York, 1973, Chap. 3, p. 135.
6. Y. Tanaka and J. Kakiuchi, *J. Macromol. Chem.*, **1,** 307 (1966).
7. A. Feltzin, M. K. Barsh, E. J. Peer, and I. Petker, *Macromol. Sci.*, **A3,** 261 (1969).
8. Y. Tanaka and H. Kakiuchi, *J. Polym. Sci.*, **A2,** 3405 (1964).
9. R. A. Fava, *Polymer* (London), **9,** 137 (1968).
10. P. G. Babayevsky and J. K. Gillham, *J. Appl. Polym. Sci.*, **17,** 6067 (1973).

Received May 21, 1976
Revised July 30, 1976